COMPDYN 2013
4th ECCOMAS Thematic Conference on
Computational Methods in Structural Dynamics and Earthquake Engineering
M. Papadrakakis, V. Papadopoulos, V. Plevris (eds.)
Kos Island, Greece, 12–14 June 2013

AN OPTICALLY BASED ASSESSMENT OF PEDESTRIAN BALANCE BEHAVIOUR WHILE WALKING ON A LATERALLY OSCILLATING TREADMILL

Seán P. Carroll, John S. Owen, and Mohammed F.M. Hussein

Centre for Structural Engineering and Construction (CSEC)
University of Nottingham
University Park
Nottingham
NG7 2RD, UK
e-mail: sean.carroll@nottingham.ac.uk
john.owen@nottingham.ac.uk
mohammed.hussein@nottingham.ac.uk

Keywords: Human-Structure Interaction, Human-Induced Vibration, Biomechanics, Amplitude Modulation, Motion Capture, Inverted Pendulum

Abstract. *This paper reports findings from an experimental campaign in which subject balance behaviour while walking on a laterally oscillating treadmill was recorded. A 3-dimensional motion capture camera system was used to track the position of 31 active markers, placed on each subject during walking tests. A range of deck oscillation frequencies and amplitudes were tested. The campaign was executed with the aim of identifying the interaction mechanism by which pedestrians produce force harmonics, that resonate with the oscillating structure on which they walk. These so-called self-excited forces have been experimentally identified by others but the underlying reason for their existence has remained an open question.*

Analysis has revealed that subject balance response to sinusoidal base motion is dominated by periodic alteration of foot placement position. This results in amplitude modulation of the lateral component of the ground reaction force (GRF). The frequency of modulation was found to be equal to the modulus of the difference between the lateral forcing and deck oscillation frequencies. This is consistent with the identification of interaction force harmonics as frequency sidebands. The underlying reason for gait width modulation was revealed by examining the subject's CoM oscillation and recognising the influence of a sinusoidally varying inertia force experienced by the subject. Furthermore, the degree to which the subject alters their gait is determined by the degree to which their frontal plane stability is impaired by deck motion. Thus the link between frontal plane balance behaviour and the generation of the self-excited component of the lateral GRF is established.

Further analysis suggests that subject centre of mass (CoM) motion while walking on a laterally oscillating deck is predominantly passive. The simple inverted pendulum model is thus an excellent model of pedestrian CoM motion in the frontal plane during the single stance gait phase. This was established by comparison between simulated and observed CoM motion.

1 INTRODUCTION

The process of step synchronisation between pedestrians and an oscillating bridge deck is now thought to be preceded by a more subtle interaction [1, 2]. This human-structure interaction (HSI) (as opposed to human-structure synchronisation) results in force harmonics within the GRF spectrum, that resonate with the bridge deck oscillation [3, 4]. Fundamental to the production of these resonant force harmonics is the pedestrian's balance response to base motion. As such, to further understand HSI, one must first consider pedestrian stability and balance behaviour during locomotion.

To this end, an experimental campaign was designed in which test subjects walk individually on a laterally oscillating treadmill. A range of tests were carried out, with varying oscillation frequencies and amplitudes imposed on the deck. GRFs were directly measured using deck mounted load cells. In addition, each subject was instrumented with 31 active visual markers in order to record 3-dimensional whole body motion.

The experimental campaign was carried out between March and May of 2012, in the Human Performance Laboratory, at the University of Nottingham. The test protocol received ethical approval from the Faculty (of Engineering) Research Ethics Committee within the University of Nottingham. The test protocol for an individual subject was as follows;

- The subject was familiarised with the oscillating treadmill rig and all safety procedures.
- The subject was instrumented with gait analysis wands and visual markers.
- The subject had a further unrecorded period of familiarisation walking on the treadmill without lateral motion, lasting approximately 10 minutes. During this time a comfortable walking speed was selected by the subject
- The subject was then recorded walking without lateral motion imposed on the deck. This data served as a baseline for the subject's walking behaviour.
- After baseline tests were completed, the subject was recorded walking while lateral oscillations were imposed on the deck, referred to hereafter as dynamic tests.
- Rest breaks were imposed every 2-3 minutes during the course of the test session.

During each test, the lateral GRF was measured directly via 4 deck mounted Zemic bending beam load cells (490 N capacity each). For the duration of each dynamic test, the lateral deck displacement and acceleration were also recorded via a linear variable differential transformer (LVDT) and Schaevitz linear servo accelerometer. A sampling rate of 250 Hz was selected for all treadmill-borne data to provide good time domain resolution. A National Instruments SCXI-1000 chassis, housing a SCXI-1100, 32 channel multiplexer amplifier (receiving LVDT and accelerometer signals) and SCXI-1520 strain bridge (receiving load cell signals) was used to coordinate data logging and signal conditioning. The chassis was also used to trigger simultaneous logging of the marker data. All marker data was sampled at 100 Hz using a CODA ActiveHub computer from Charnwood Dynamics Ltd.

Five oscillation amplitudes were tested, 5 mm, 10 mm, 20 mm, 35 mm and 50 mm. Within each amplitude, 9 oscillation frequencies were tested ranging from 0.3 Hz to 1.1 Hz in 0.1 Hz increments, resulting in a 45 point test matrix.

Ten subjects took part in the test campaign. The age, height and weight of all participants is shown in table 1. The majority of anthropometric data in the literature has been obtained from

male subjects. In order to utilise this data as effectively as possible only male subjects were recruited for this campaign. This is justifiable when one considers that there is no reason to suspect that male subjects will behave (statistically) significantly differently to female subjects. It is therefore assumed (until proven otherwise) that the behaviours observed and conclusions drawn are equally applicable to both sexes.

Table 1: Test subject data.

Subject	Height (m)	Mass (kg)	Age (Years)
1	1.73	82.05	28
2	1.82	96.20	30
3	1.74	63.05	27
4	1.84	98.95	28
5	1.68	85.45	34
6	1.88	90.95	21
7	1.82	87.20	26
8	1.61	75.00	31
9	1.80	74.05	28
10	1.76	82.70	34
Mean	1.77	83.11	28.7

2 OSCILLATING TREADMILL

The design of the treadmill test rig, Fig. 1 (a), is similar to that originally constructed by Pizzimenti [5] and used more recently by Ingólfsson [4]. What marks this test campaign as a further development of what has gone before is the use of motion capture techniques and the focus on the biomechanical behaviour that is ultimately responsible for GRF generation.

2.1 Construction

The treadmill structure consists of three steel frames arranged as follows (refer to Fig. 2):

1. The base frame is the lowermost frame and remains stationary. The motor providing lateral motion is connected to this frame.

2. The chassis frame sits on 4 carriages that travel along linear guide rails fixed to the base frame. The chassis frame is driven laterally by a drive arm connected to the motor, see Fig. 1 (b). Thus rotational motion, provided by the motor is converted, through the drive arm, to sinusoidal reciprocating motion.

3. The uppermost treadmill frame is suspended from the chassis frame by 4 hangers, Fig. 1 (c). The self-weight of the treadmill frame and any vertical imposed loads are resisted by the hangers. The treadmill frame is restrained laterally by 4 bending beam load cells, the means through which the lateral GRF is recorded. The treadmill belt is driven by a second motor mounted on the chassis frame.

The chassis frame is driven laterally by a Nordbloc 0.55 kW geared motor. A specifically designed coupling is used to allow the drive arm to be fitted at different radii from the motor

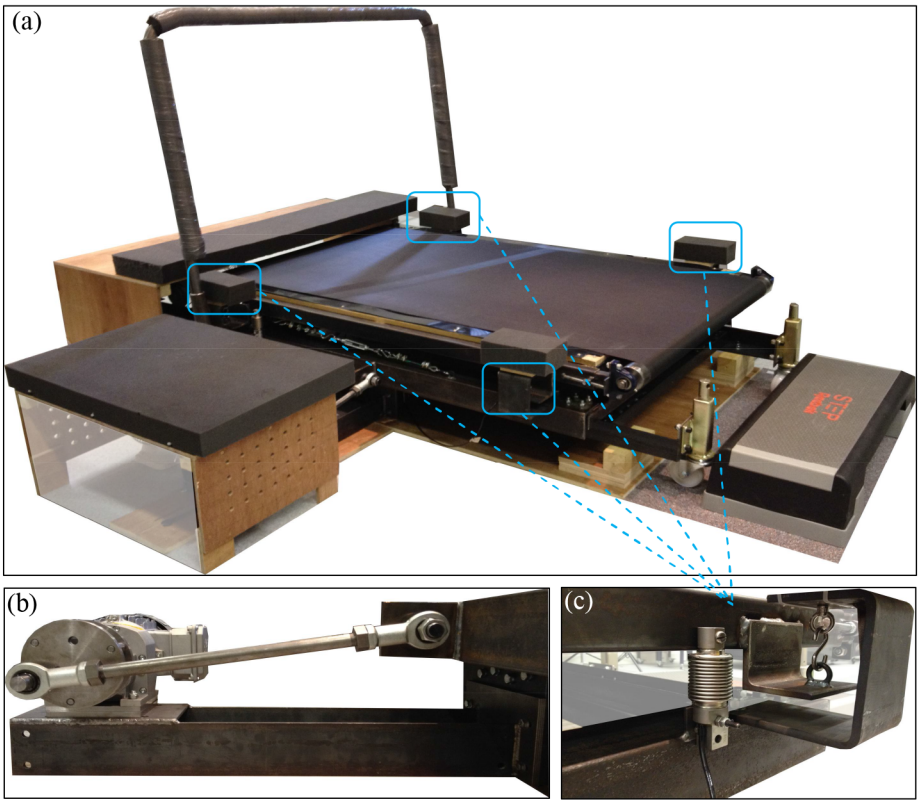

Figure 1: (a) Oscillating treadmill test rig, (b) Motor and lateral drive arm producing reciprocating sinusoidal motion from rotary motion, (c) Hanger and load cell arrangement (1 of 4), the treadmill deck is supported vertically by hangers and restrained laterally by bending beam load cells.

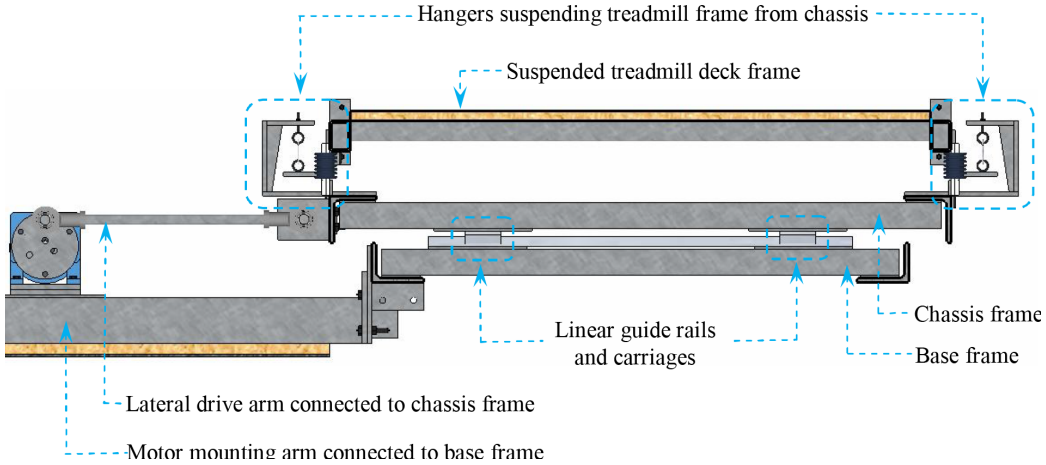

Figure 2: Section through treadmill rig showing three constituent frames (base, chassis and treadmill deck), lateral drive system, and lateral restraint of treadmill deck frame against chassis frame.

shaft, allowing variability in the deck oscillation amplitude. The treadmill belt is itself belt driven by a Nordbloc 0.75 kW geared motor. The speed of both motors is controlled via 2 Siemens G110 inverters.

The deck walking area measures 1 m wide $\times$ 1.5 m long. A horizontal bar/handle was placed across the front of the treadmill to provide extra stability should a test subject feel particularly unstable. Subjects were instructed not to touch the bar unless absolutely necessary, after which

the test data was discounted. The front-mounted bar is obviously not in keeping with what one would experience on a real bridge, however side rails could not be provided without obscuring marker visibility.

2.2 Data acquisition and rig validation

The accelerometer and LVDT recording deck motion were digitally low pass filtered with 4th order Butterworth (BW4) filters with cutoff frequencies of 5 Hz and 2 Hz respectively. The load cells were digitally low pass filtered at 6 Hz (BW4). The lateral GRF obtained from the treadmill rig shall be referred to as the measured GRF, $F_{L,meas}$, and is calculated as,

$$F_{L,meas} = \left(\sum_{i=1}^{4} F_{c,i} \right) - m_d \, \ddot{U}_d \tag{1}$$

in which $F_{c,i}$ is the load imposed on the i^{th} load cell, m_d is the mass of the treadmill deck and associated suspended structure and $\ddot{U}_d$ is the lateral acceleration of the treadmill deck. $F_{L,meas}$ was validated against GRFs recorded from independently calibrated Kistler force plates (in-situ in the Human Performance Lab). It is obviously not possible to directly compare forces from the same footstep, therefore the modified force plate record is compared against the phase-averaged cycle obtained from the treadmill, Fig. 3. Further discussion of rig force data processing can be found in [6]. Allowing for the time domain effects of intra-subject variability, good agreement is observed between treadmill and force plate data. This provides confidence that GRFs are being extracted from the test rig with acceptable accuracy.

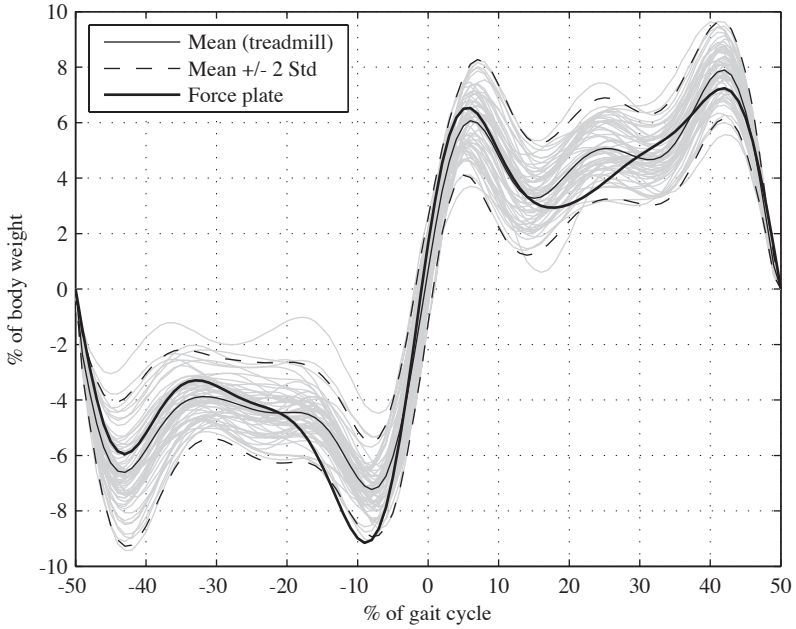

Figure 3: Comparison between the resultant lateral GRFs determined from the treadmill and from the laboratory force plates. Treadmill GRFs from multiple gait cycles are plotted along with the sample mean and $\pm$ 2 standard deviation boundaries.

3 MOTION CAPTURE SYSTEM

A Coda mpx30 general-purpose 3D motion tracking system was used. The system consists of 2 measurement units, each containing 3, pre-aligned cameras, wall mounted on either side

of the treadmill deck. The cameras track the position of active markers (infra-red LEDs) in the measurement volume, achieving a position resolution of 0.1 mm horizontally and vertically and a distance resolution of 0.3 mm. Each subject was instrumented with 31 active markers, placed directly on the skin (over bony landmarks) and attached to gait analysis wands strapped to the body, Fig. 4. The use of gait analysis wands improves marker visibility and facilitates the calculation of joint centres and body segment embedded vector bases (EVB).

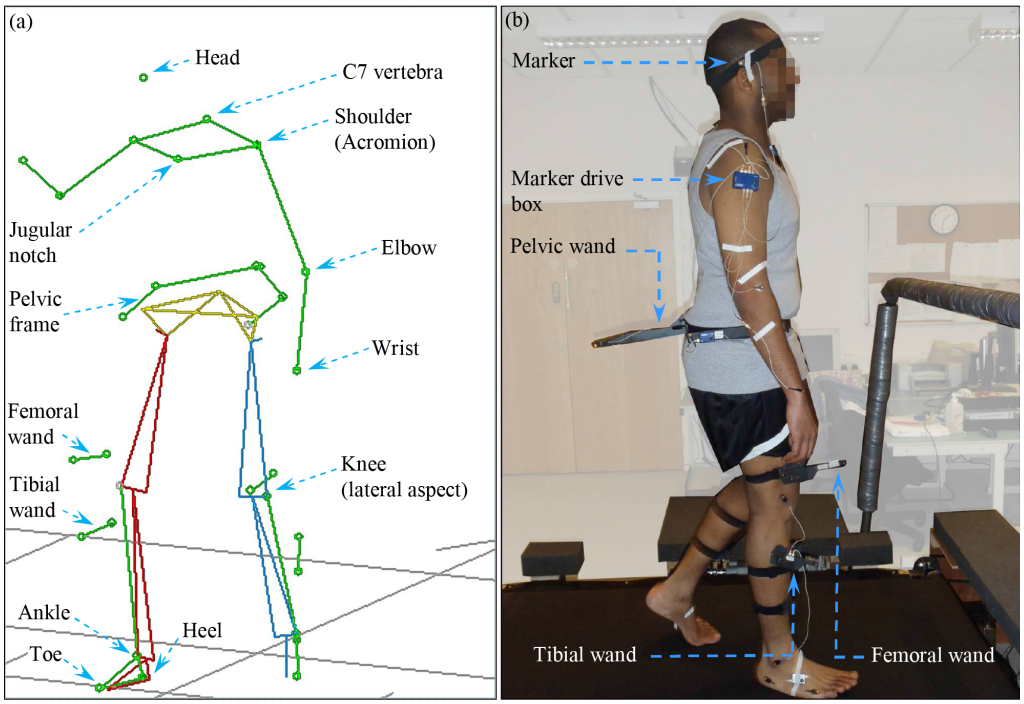

Figure 4: (a) Marker arrangement showing locations of 31 active markers, (b) Test subject instrumented with markers and gait analysis wands.

3.1 Marker placement

During testing subjects wore a sleeveless shirt and shorts, Fig. 4 (b). Subjects were not permitted to wear any form of footwear. This may at first appear odd as pedestrians walking on a bridge rarely walk barefoot. However, the emphasis in this campaign is on understanding biomechanical response in the face of lateral deck motion. The somatosensory information received through the sole of the foot is undoubtedly altered if a person wears shoes. Whether or not this information is altered to the extent that it has an influence on the actual balance behaviour is less certain. It was therefore decided to remove any potential variability introduced by footwear.

The positioning of all markers placed at or below hip level was determined by the marker placement protocol set out in the Coda mpx30 user guide [7]. Hip, knee and ankle joint centres are calculated relative to marker positions as per the procedure set out in [7]. Markers placed on the upper torso, arm and head were placed based on the specific requirements of this test campaign; to allow quantification of upper torso rotation and head and arm movement allowing accurate calculation of the CoM trajectory.

More specifically, markers were positioned at the heel, at the end of the 5^{th} metatarsal (toe), both facing laterally, at the lateral malleolus (ankle) and on the lateral aspect of the medio-lateral

knee axis. Tibial and femoral wands, containing two additional markers each, were strapped to the subject's lower leg and thigh.

A pelvic frame containing 6 markers allows a pelvis EVB to be constructed. Two markers were positioned such that they formed an imaginary line passed through the anterior superior iliac spine (ASIS markers), two more were positioned similarly for the posterior superior iliac spine (PSIS markers). Two more were placed on either side of a wand extended from the sacrum.

Four markers were placed to allow the construction of an EVB for the upper torso; one on each acromion (shoulder), one over the C7 vertebra at the back of the neck and one over the jugular notch. An additional marker was also placed just above the ear, at eye level. Finally, a marker was placed on the lateral aspect of each elbow and wrist in order to record arm movement.

4 GAIT BEHAVIOUR AND THE SELF-EXCITED FORCE

The self-excited (SE) force and its equivalent mass and damping effects have been investigated previously. However, the biomechanical behaviour resulting in the GRF, of which the SE force is a part, has not been sufficiently explored. The equipment and techniques employed in this investigation allow whole body behaviour of the test subject to be observed. As such, a more complete picture of HSI is obtained.

The following two figures detail the behaviour of subject 1 during individual dynamic tests and demonstrate the salient behaviours observed. Further discussion of this data can be found in [6]. The imposed deck oscillation amplitude is 10 mm and deck oscillation frequencies are 0.7 Hz and 0.9 Hz. In both cases the subject maintained a constant pacing frequency of 1.8 Hz, resulting in a lateral forcing frequency of 0.9 Hz throughout the tests.

Figure 5 (a) shows the subject's CoM oscillation relative to the moving deck (solid black line and left scale), the corresponding deck oscillation is also shown (solid grey line and right scale). The underlying deck motion has been removed from all marker data, thus all reported subject motion is relative to the moving deck. Markers on the lateral aspect of the foot, at the heel and toe have been used to determine the position of the foot for each footstep (intermittent black lines), the position is calculated as the median point between both markers. The circle at each foot position, marks the average foot position for the duration of the footstep.

Plot (b) shows the step widths for successive steps, defined as the lateral distance between the mean foot position marks. The x-axis position of each vertical stem is determined as the mid-time between the foot positions used to calculate that step width. Plot (c) shows the directly measured GRF, $F_{L,meas}$, and plot (d) shows its harmonic components.

The most striking feature of the subject's behaviour is the alteration of their gait width. Closer inspection of plot (a) reveals that if the subject steps to the left in time with the rig's maximum leftward displacement (and vice versa on the right), the CoM oscillation amplitude is a minimum. Conversely, when the subject steps in a direction opposite to the deck's motion and in time with the peak deck displacement, the CoM amplitude is at a maximum. This is a direct result of the sinusoidally varying inertia force experienced by the subject due to the base acceleration. Owing to the different pacing and oscillation frequencies, this results in a periodic modulation of the CoM oscillation amplitude. Coincident with this, is a narrowing and widening of the subject's gait and as a result, modulation of the GRF occurs.

When the whole body behaviour responsible for the GRF is examined, it becomes apparent that the gait width and therefore the GRF is being modulated at a fixed frequency equal to the modulus of the difference between the lateral forcing frequency and the base oscillation

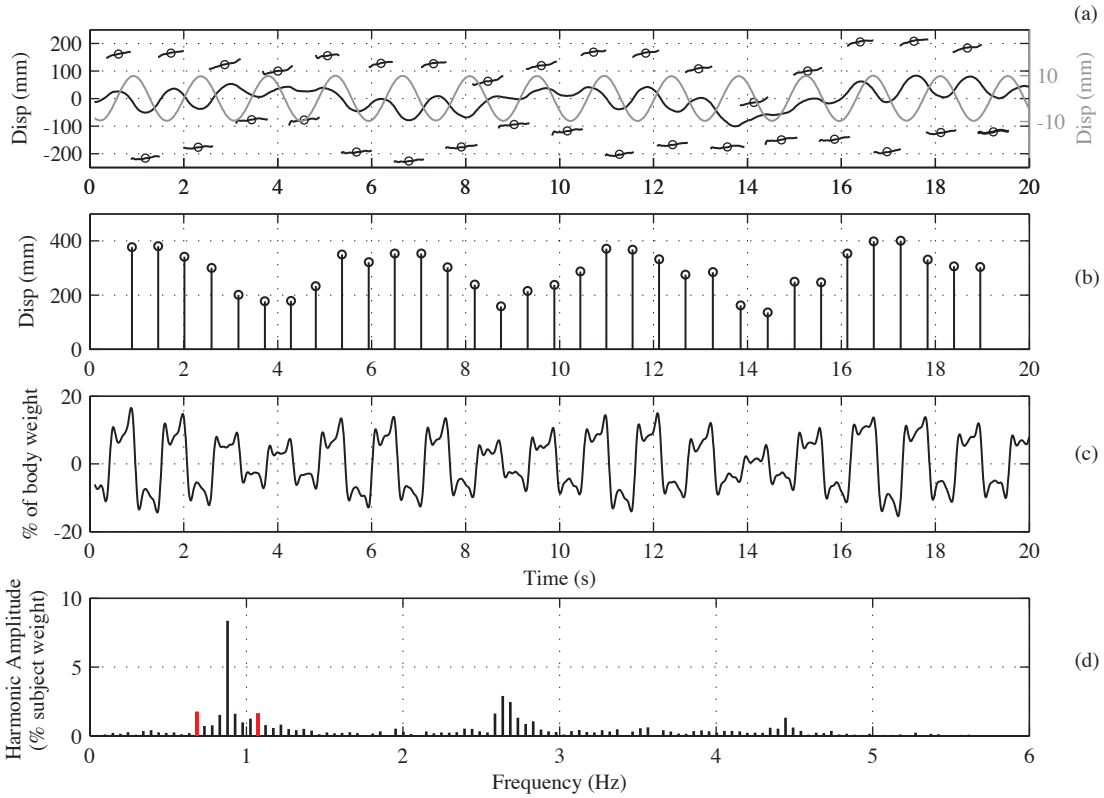

Figure 5: Deck oscillation amplitude = 10 mm, frequency = 0.7 Hz. (a) CoM oscillation (continuous black line and left scale), deck oscillation (continuous grey line and right scale) and lateral foot position (intermittent black line), (b) step widths, (c) directly measured GRF, (d) harmonic components of the directly measured GRF (interaction forces shown in red).

frequency, in this case approximately 0.2 Hz or every 5 seconds. The gait width modulation is quantified through the percentage modulation depth, MD, where:

$$\text{MD} = 100 \times \frac{\text{wave peak} - \text{wave trough}}{\text{wave peak} + \text{wave trough}} \tag{2}$$

The wave peak was determined by discarding the maximum value of gait width and obtaining the average of the next two largest values. The corresponding procedure was applied to the minimum gait widths to determine the wave trough. In the case of Fig. 5, MD $= 42\%$

Plot (d) shows the harmonic components of the GRF, the interaction force harmonics are shown in red. Notably, these are also spaced approximately 0.2 Hz on either side of the fundamental force harmonic, a measure predicted by the biomechanical behaviour described above.

In Fig. 6, the base oscillation amplitude is 10 mm but the frequency is increased to 0.9 Hz, synchronised with the lateral forcing frequency imposed by the subject. The alterations in gait width previously observed are notably absent, plot (a) and (b). CoM oscillation amplitude, gait width and GRF amplitude all remain relatively stable during the test. Due to the constant phase relationship between the subject's lateral forcing frequency and the deck oscillation frequency, the inertia force experienced by the subject remains the same from gait cycle to gait cycle. This eliminates the need to periodically alter foot placement position to maintain frontal plane stability, instead, the subject adopts a wider gait sufficient to deal with the imposed inertia force, leading to a scale increase in the GRF.

To investigate the generality of this frequency relationship, the factor β is defined as the ratio

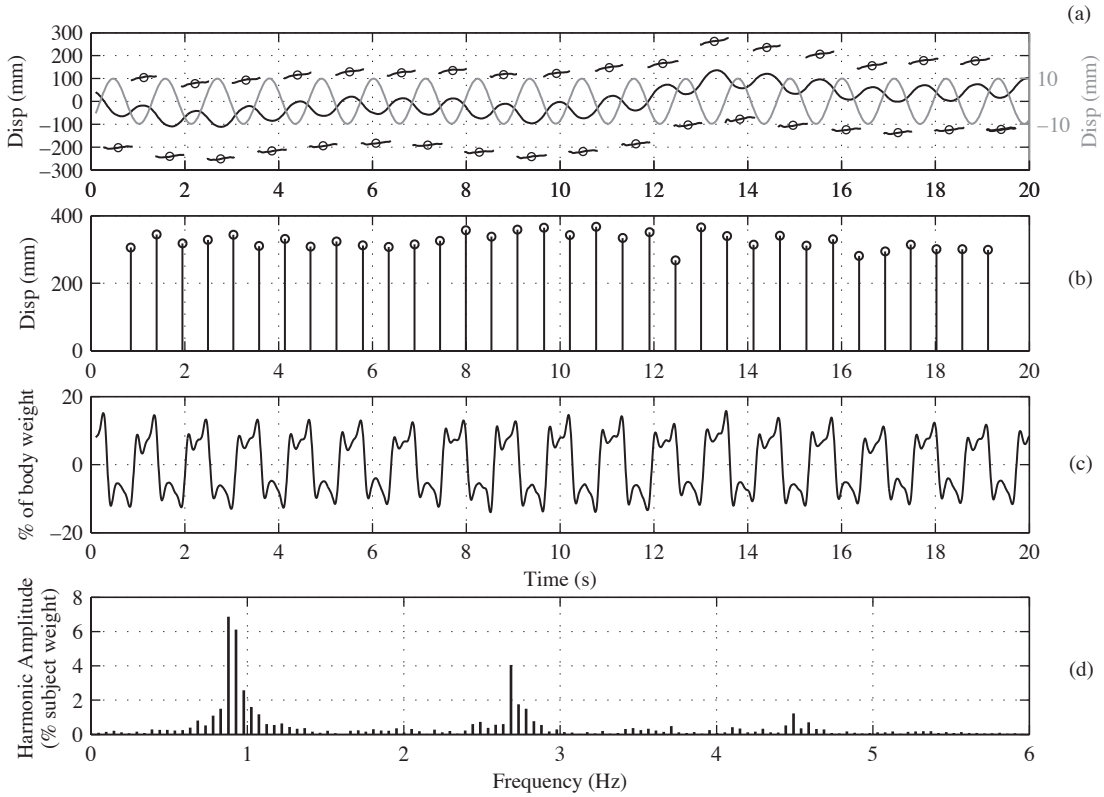

Figure 6: Deck oscillation amplitude = 10 mm, frequency = 0.9 Hz. (a) CoM oscillation (continuous black line and left scale), deck oscillation (continuous grey line and right scale) and lateral foot position (intermittent black line), (b) step widths, (c) directly measured GRF, (d) harmonic components of the directly measured GRF.

of observed modulation frequency to the modulation frequency predicted by the base oscillation and forcing frequency relationship:

$$\beta = \frac{\text{Observed modulation frequency}}{|f_{\text{base}} - f_{\text{subject}}|} \tag{3}$$

where f_{base} is the base oscillation frequency and f_{subject} is the frequency of the lateral GRF imposed by the subject (0.9 Hz). Figure 7 show the ratio β calculated for each test completed by subject 1. Note that β values for which $f_{\text{base}} \approx f_{\text{subject}}$ have been omitted as the parameter is not applicable under this frequency regime.

It can be seen that in the majority of cases $\beta \approx 1$, indicating that a periodic gait width modulation is generally occurring at a frequency equal to $|f_{\text{base}} - f_{\text{subject}}|$. The biomechanical motivation for alteration of foot position has been identified as being a response to a sinusoidally varying inertia force. Furthermore, the frequency of the SE force harmonic is also identified as $f_{\text{subject}} \pm |f_{\text{base}} - f_{\text{subject}}|$. Therefore, Fig. 7, in which β is predominantly equal to one, establishes the link between pedestrian balance behaviour and the generation of a SE force harmonic.

Note that for the lowest frequency test during 5 mm and 10 mm amplitude oscillations, Fig. 7 plots (a) and (b), $\beta \approx 0$. This is due to the gait width modulation not being sufficiently well defined for a dominant harmonic to be extracted. In both cases the peak lateral acceleration experienced by the subject < 0.04 m/s^2 and resulted in only a minor influence on gait width. However as the strength of external stimulus grows, periodic modulation is quickly established.

The percentage MD and normalised average gait width have been determined for each test completed by subject 1, Fig. 8. The average gait width has been normalised by the average

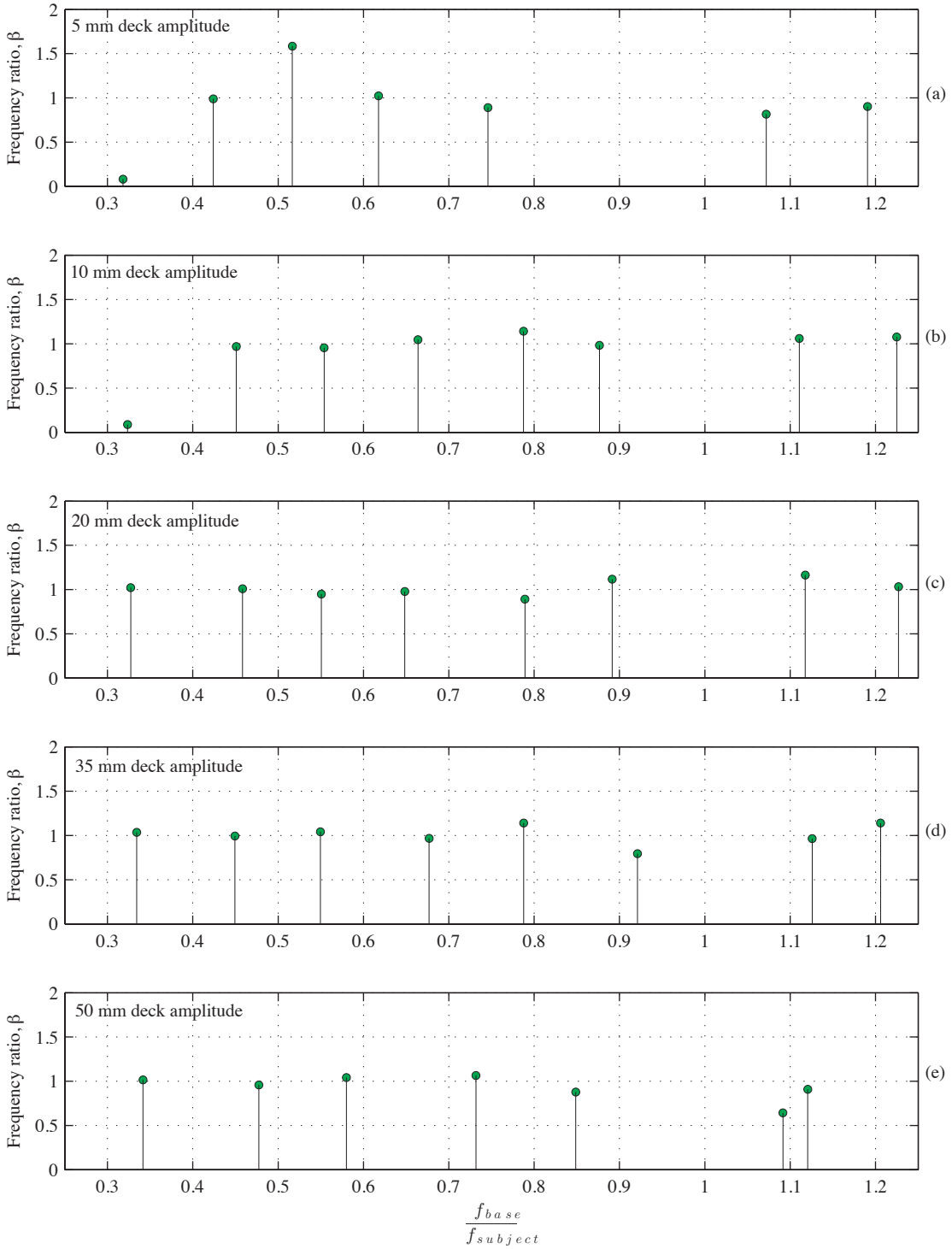

Figure 7: The ratio of observed gait width modulation frequency to that predicted by the expression, $|f_{\text{base}} - f_{\text{subject}}|$. Data shown for 5 mm (a), 10 mm (b), 20 mm (c), 35 mm (d) and 50 mm (e) amplitude tests, completed by test subject 1.

obtained for the subject during static (treadmill) tests.

During 5 mm amplitude tests, Fig. 8 (a), MD is relatively low ($< 20\ \%$), although this increases as the deck oscillation frequency increases imposing higher amplitude oscillations on the subject. Interestingly, despite the low oscillation amplitude, the mean gait width is

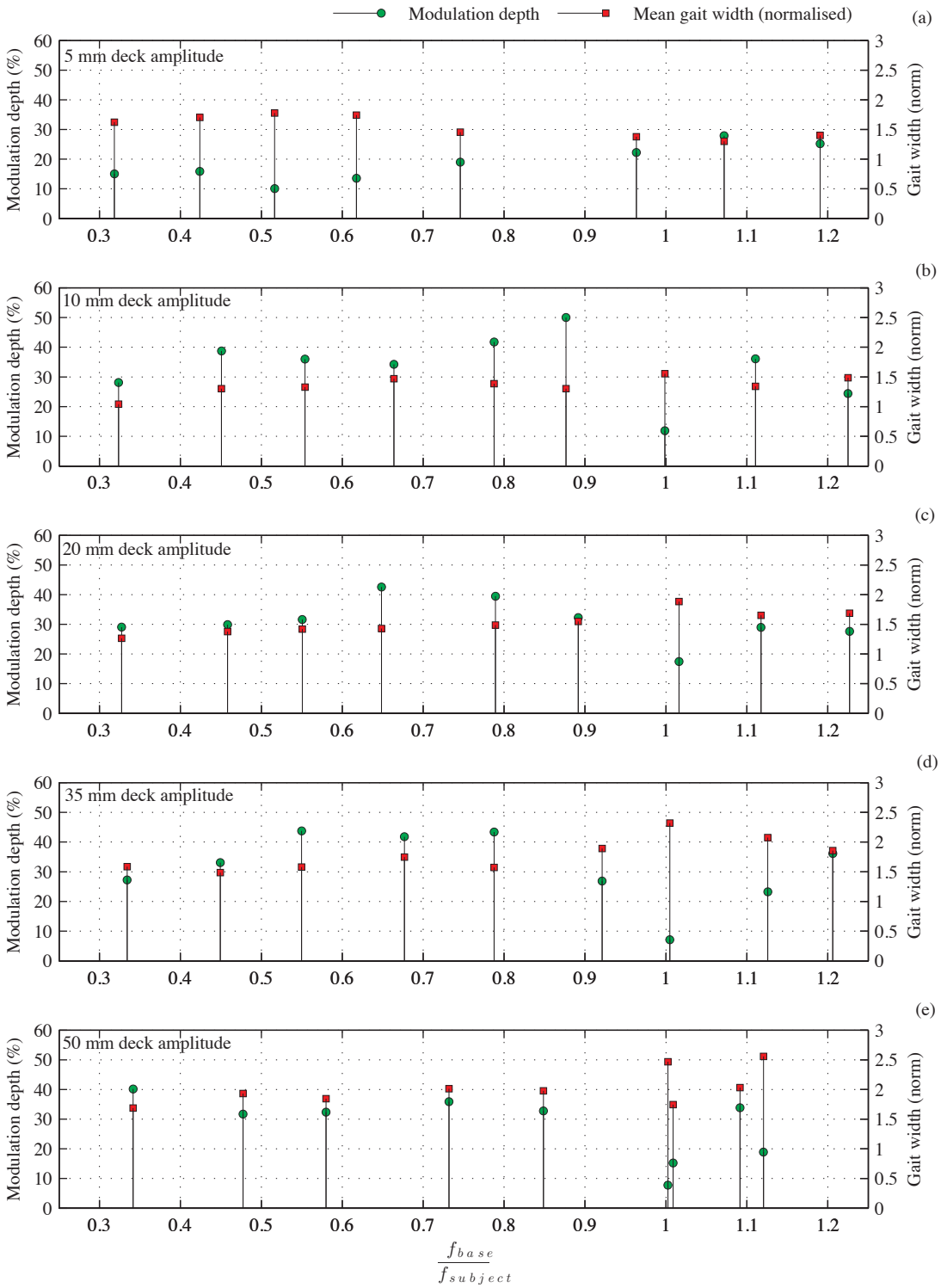

Figure 8: The percentage MD and normalised average gait width for each test completed by subject 1. Data shown for 5 mm (a), 10 mm (b), 20 mm (c), 35 mm (d) and 50 mm (e) amplitude tests.

approximately 50% greater than that observed during static tests. This underlines the subject's sensitivity to frontal plane motion.

During larger amplitude oscillations, MD increases and is generally in excess of $30\,\%$ and in some cases $40\,\%$. The gait width ratio remains stable at approximately 1.5 for 5 mm, 10 mm

and 20 mm tests. However it increases significantly for 35 mm and 50 mm tests.

The stabilisation of gait width discussed previously is clearly seen for cases when the subject is synchronised with the deck. In all cases when $(f_{\text{base}}/f_{\text{subject}}) \approx 1$, MD is reduced significantly. In such cases the average gait width is typically wider than for unsynchronised walking. Figures 7 and 8 have demonstrated that the detailed discussion presented above for subject 1 does indeed represent typical gait behaviour for that subject. Furthermore, the behaviour identified above, was found to be typical across all test subjects, although there was significant quantitative inter-subject variability.

5 PASSIVE VERSUS ACTIVE CoM MOTION

To investigate subject CoM motion (in the presence of the deck-induced inertia force), a simple comparison between observed subject behaviour and that predicted by an equivalent passive inverted pendulum (IP) model was considered, Fig. 9. Data relating to subject number 4 is discussed in detail herein.

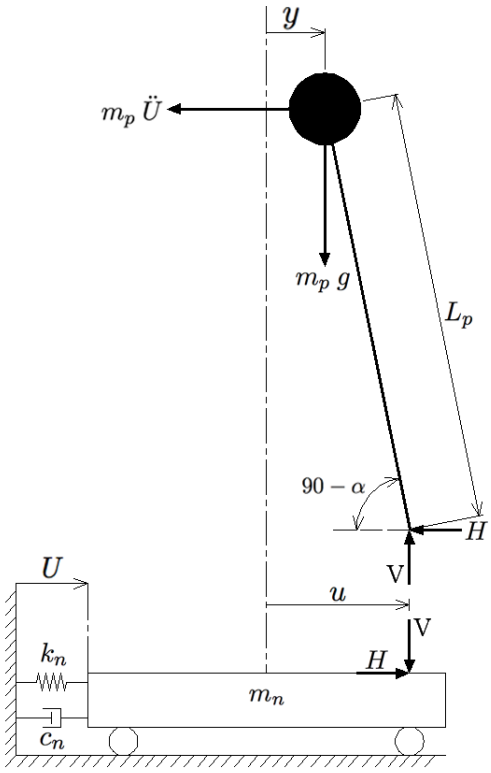

Figure 9: Biomechanical IP model on a laterally moving structure.

To facilitate the comparison, an IP model equivalent to the subject in question was established. The IP length was determined as the vertical distance to the subjects CoM (based on marker data and de Leva's body model [8]), while the IP mass was equal to the subject's body mass. The IP walking model, stabilised by the support placement law given by Eq. (4) [9], was subjected to the same base motion experienced by the subject. Its motion was them compared with the subject's observed CoM motion, reproduced from marker data.

$$u = y_0 + \frac{\dot{y}_0}{\omega} \pm b_{min} \tag{4}$$

IP support position, u, is determined by the IP mass position, y_0, and velocity, $\dot{y}_0$, immediately before the 'foot' is placed. The IP biomechanical model and its implementation as a pedestrian model in the study of HSI is discussed in detail in [10, 11, 12, 13], to which the reader is referred for further IP model background information.

5.1 IP-subject comparison: Stationary deck

The IP was first tuned to match the subject's observed behaviour during a stationary test in which no treadmill oscillation was imposed. IP initial mass position, velocity and support position were chosen to match the subject at the beginning of the simulation. In order to tune the IP behaviour to match the subject, the minimum stability margin, b_{min} from Eq. (4) was used as a tuning parameter.

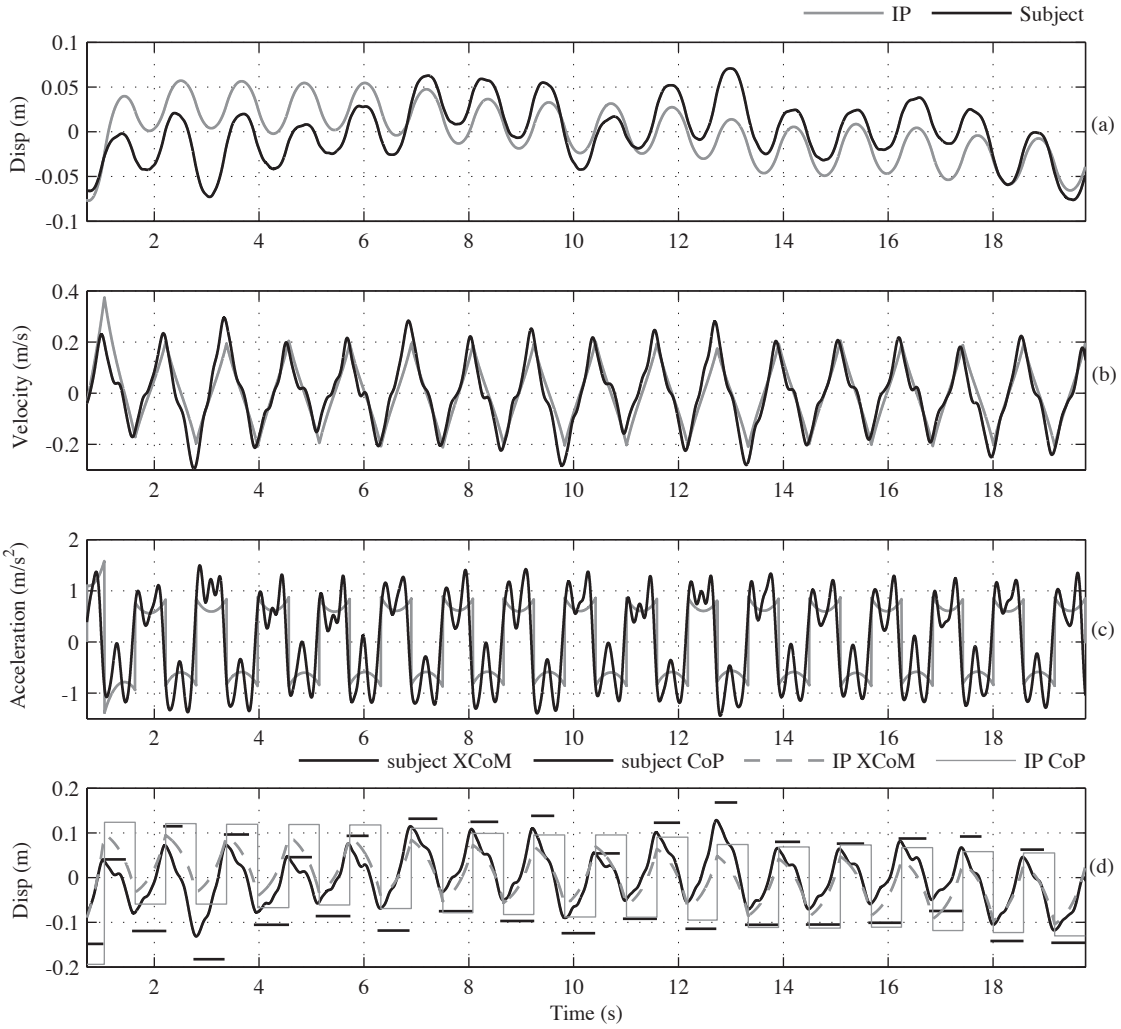

Figure 10: Comparison between subject and equivalent IP, (a) CoM position (correlation coefficient, CC = 0.55, slope of the linear regression line, m$_{reg}$= 0.51), (b) CoM velocity (CC/m$_{reg}$ = 0.93/0.77), (c) CoM acceleration (CC/m$_{reg}$ = 0.81/0.66) and (d) XCoM and CoP position.

The cumulative area under the (absolute) GRF time history was compared for the IP and subject and b_{min} altered until the difference in areas was a minimum. Note that the subject's measured rather than reproduced GRF was considered. Figure 10 shows the result of this tuning

process for CoM position, velocity and acceleration, plots (a) to (c). Plot (d) shows a comparison between extrapolated centre of mass (XCoM) and centre of pressure (CoP) position for the subject and IP.

The initial drift in IP CoM trajectory results from a discrepancy between the IP and subject's (assumed) initial CoP position. The influence of this discrepancy is dissipated within the first two steps and has no bearing on the comparison thereafter. To facilitate the comparison, the mean value offset (determined after the first two steps have occurred) has been removed from both sets of data in plot (a). This removes the influence of the initial drift in simulated CoM motion, arising due to the initial CoP position inaccuracy. The same offsets have also been removed from the simulated and observed data in plot (d).

Considering the CoM position, velocity and acceleration comparisons in plots (a), (b) and (c), the IP appears to simulate the CoM trajectory quite well, particularly in the case of the CoM velocity, plot (b). With reference to plot (a), it is apparent that the IP model is unable to simulate 'atypical' CoM oscillations such as arise from the subject drifting across the treadmill deck as they walk. Nevertheless, the general character of the oscillatory behaviour agrees quite well. The CoM accelerations in plot (c) show good amplitude agreement (ensured by the b_{min} tuning process), although the subject's acceleration during the mid-stance deviates significantly from the smooth trajectory simulated by the IP.

Plotting the simulated versus observed behaviour for position, velocity and acceleration data, the correlation coefficient (CC) is used as a quantitative measure of the linearity between simulated and observed behaviour. In this way, linearity is used as the measure of similarity. These were calculated as 0.55, 0.93 and 0.81 for position, velocity and acceleration respectively. However, this measure is independent of any scaling difference between simulated and observed trajectories. This is quantified by the slope of the line of linear regression, m_{reg}, between observed and simulated behaviour. These are calculated as 0.51, 0.77 and 0.66, all identifying that the magnitude of position, velocity and acceleration is underestimated by the IP model. In this way, the simulated versus observed comparison (averaged for the duration of the comparison) is represented by two parameters, CC, representing linearity and m_{reg}, representing purely scale differences.

Plot (d) shows the XCoM and CoP positions for the subject and IP. A constant medial offset of 35 mm has been applied to the recorded foot position to approximate the average position of the subject's CoP. Again, with the exception of anomalous steps, eg. at t = [3, 5, 13] s, the IP approximates the subject's behaviour well. Considering the complexity of human locomotion and the comparative simplicity of the biomechanical model, the general agreement seen in Fig. 10 is encouraging. Particularly considering the IP model's prevalence in the study of HSI.

5.2 IP-subject comparison: Oscillating deck

Having tuned the IP model to the specific subject under consideration, the comparison is now repeated for dynamic tests. If the model performs well, it can be concluded that subject CoM oscillation is predominantly passive and any active balance control in response to deck motion can be discounted. However, if there is a divergence in the predicted and observed balance behaviour, the alternative conclusion can be drawn, i.e. that there is some form of additional active control causing the subject to behave differently to the passive pendulum.

Figures 11 and 12 represent two dynamic test comparisons which indicate the IP model's performance. In both cases the subject's lateral forcing frequency was approximately 0.9 Hz. When determining the IP support placement position from Eq. (4), the CoM velocity relative to the moving deck was found to be appropriate.

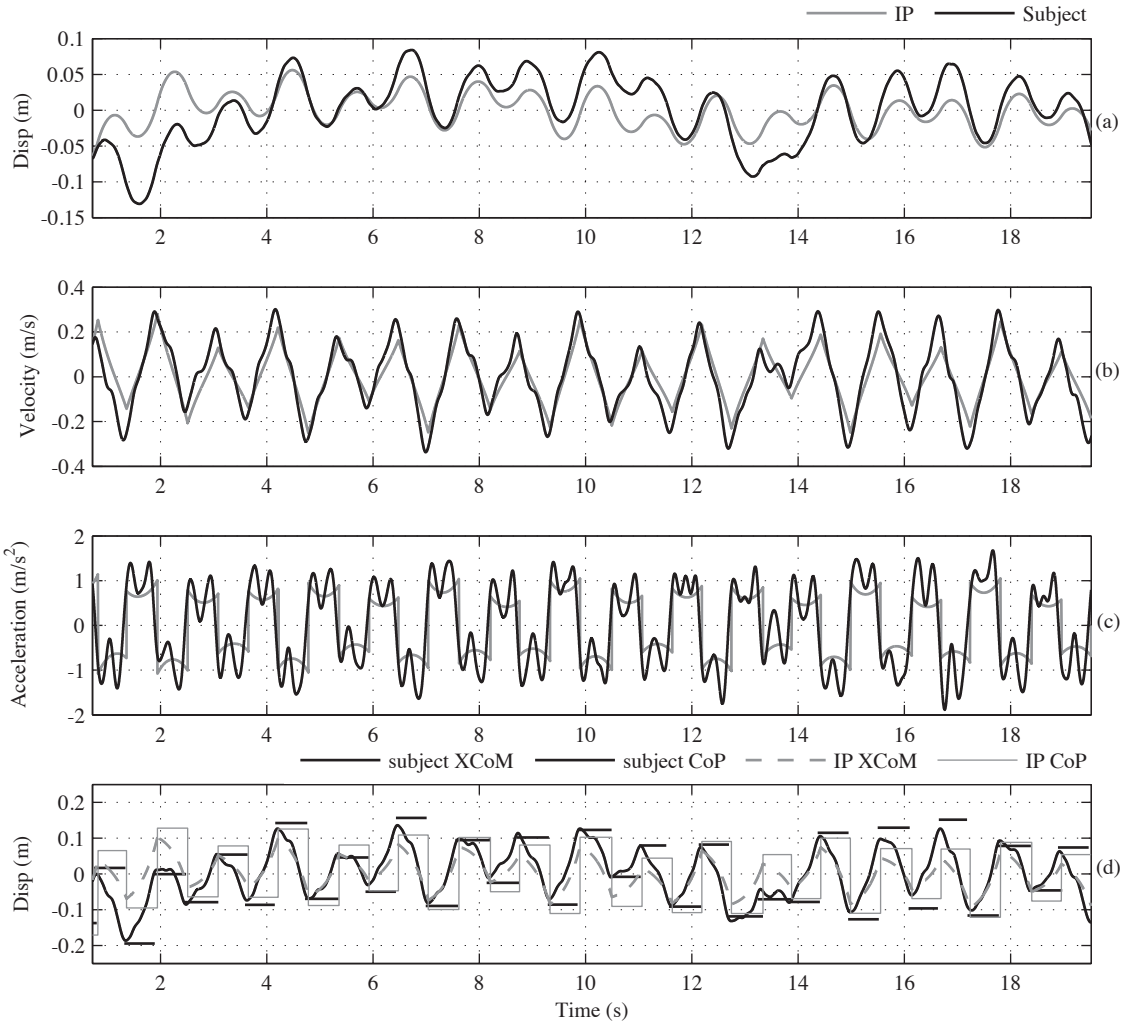

Figure 11: Comparison between subject and equivalent IP, deck oscillation 10 mm amplitude at 0.5 Hz. (a) CoM position (CC/m$_{reg}$ = 0.64/0.34), (b) CoM velocity (CC/m$_{reg}$ = 0.93/0.66), (c) CoM acceleration (CC/m$_{reg}$ = 0.81/0.59) and (d) XCoM and CoP position.

Figure 11 shows the comparison during lateral oscillations of 10 mm amplitude at a frequency of 0.5 Hz. The passive dynamics of the IP appear to predict reasonably well the subject's oscillatory behaviour in the presence of deck motion. This is particularly the case between $4s <= t <= 12s$, during which position, velocity and acceleration are well predicted. However atypical behaviour, e.g. between $13s <= t <= 14s$ obviously cannot be predicted by the IP. The correlation and regression data was calculated as CC/m$_{reg}$ = 0.64/0.34 (pos), 0.93/0.66 (vel) and 0.81/0.59 (acc). It can be seen in plot (d) that the support placement law, Eq. (4), also results in modulation of the simulated gait with, broadly in line with the subject's behaviour.

Figure 12 shows the IP performance when the lateral forcing and deck oscillation frequencies coincide. The oscillation amplitude and frequency are 20 mm and 0.9 Hz respectively. Exceptionally good agreement is observed between the subject and IP behaviour, quantified by the correlation and regression data, CC/m$_{reg}$ = 0.89/0.78 (pos), 0.97/0.93 (vel) and 0.88/0.89 (acc).

As already discussed in relation to test subject 1, Fig. 6, there is a constant phase relationship between the lateral forcing and deck oscillation frequencies. As a result the inertia force experienced by the subject and IP, at the time of support placement, remains constant from gait

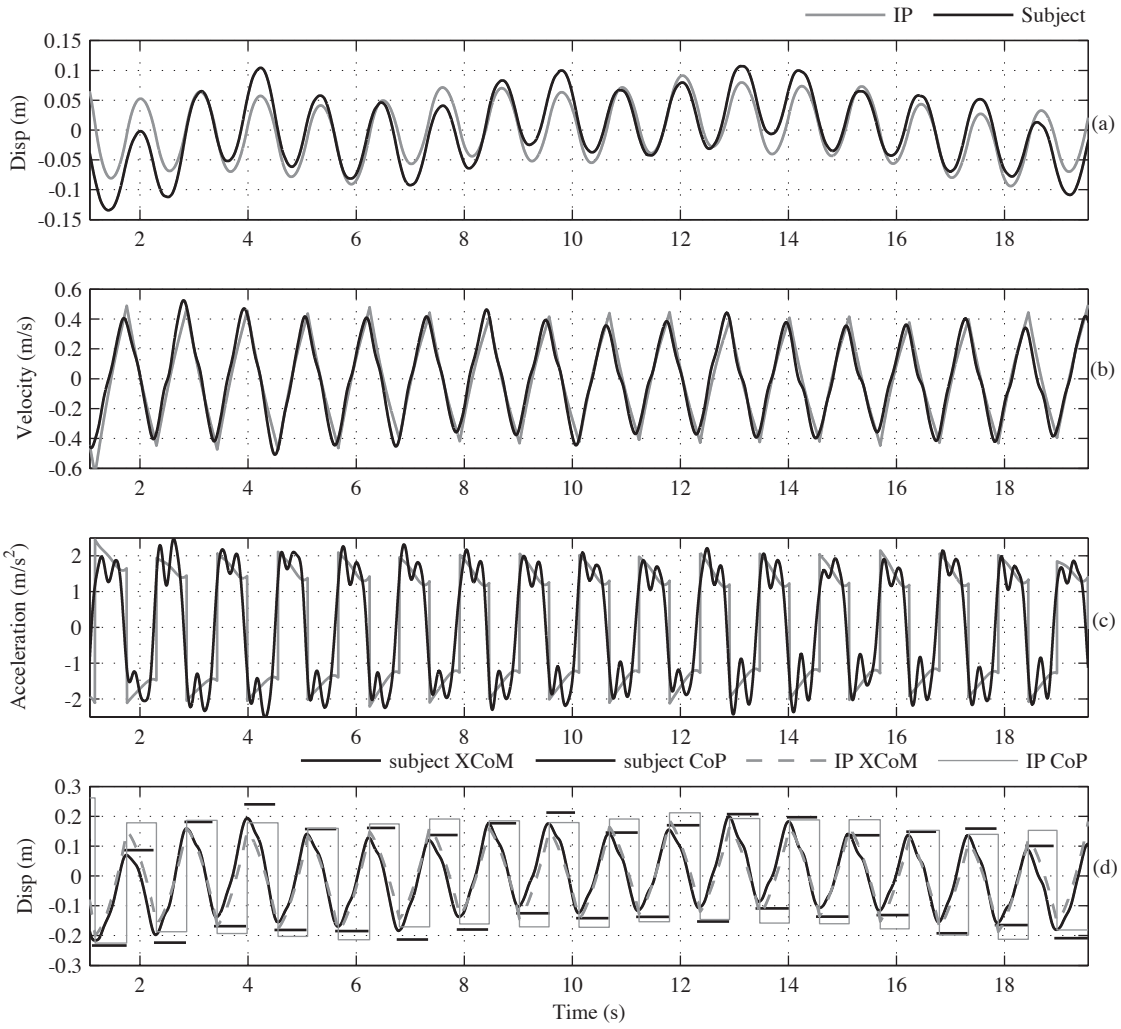

Figure 12: Comparison between subject and equivalent IP, deck oscillation 20 mm amplitude at 0.9 Hz. (a) CoM position (CC/m$_{reg}$ = 0.89/0.78), (b) CoM velocity (CC/m$_{reg}$ = 0.97/0.93), (c) CoM acceleration (CC/m$_{reg}$ = 0.88/0.89) and (d) XCoM and CoP position.

cycle to gait cycle and there is no modulation of gait width. In this particular case, the CoP position is well predicted by the balance law, Eq. (4), and as a result the CoM position, velocity and acceleration are also well predicted.

Not withstanding the inaccuracies in support placement position, exemplified by Fig. 11, Fig. 12 further confirms the suitability of a passive model for CoM oscillatory behaviour. It is at least reasonable to suggest that the passive nature of the IP model is sufficient to describe the subject's CoM oscillation in the presence of lateral deck motion. That is to say, the addition of a further active control element on CoM motion does not appear to be warranted. On this basis (and considering that similar behaviour is observed across all subject comparisons), it can be tentatively concluded that while active balance control certainly plays a role in maintaining stability during locomotion on a laterally oscillating deck, the CoM behaviour is adequately described by the dynamics of a passive IP.

A limitation of the CoP placement law, becomes apparent as the magnitude of deck velocity experienced by the IP grows. According to Eq. (4), the lateral position of the CoP contains a term proportional to CoM velocity, $\frac{\dot{y}_0}{\omega}$, and the additional stability margin, b_{min}. In the event that the IP and deck have global velocities (velocities measured in the stationary global reference

frame) in the same direction but the deck velocity magnitude is greater than the absolute velocity of the IP, the velocity of the IP relative to the deck will be in the medial direction. As a result, the term $\frac{\dot{y}_0}{\omega}$ will be opposite in sign to b_{min}. As deck velocity magnitude increases, b_{min} is effectively eroded by $\frac{\dot{y}_0}{\omega}$ and a 'crossover' step occurs. A crossover step describes the situation in which the IP CoP is placed on the 'wrong' side of the CoM for the imminent step. This behaviour, although ensuring IP stability, signals the breakdown of the balance law as the IP behaviour no longer resembles human locomotion. For this reason, comparisons have not been presented for 35 mm and 50 mm amplitude tests.

5.3 IP-subject comparison: 5 mm, 10 mm and 20 mm tests

Comparison data from all tests for subject 4 can be seen in Fig. 13 which show the subject versus equivalent IP behaviour for CoM position (plot a, d, g), velocity (plot b, e, h) and acceleration (plot c, f, i). All comparison data has been combined for 5mm tests (plots a - c), 10mm tests (plots d - f) and 20mm tests (h - i). As above, IP CoP placement is based on CoM velocity in the moving treadmill (local) reference frame.

Figure 4 demonstrates that the behaviours and level of agreement discussed above are typical for the entire text matrix for subject 4. In all cases the slope of the regression lines show that the magnitude of CoM motion is underestimated by the IP model, however in the case of velocity and acceleration, all CCs are ≥ 0.77 indicating strong linearity. CoM position however shows weaker linearity with CC between 0.36 and 0.42. This is due to the tendency for the subject (and IP) to drift laterally on the deck during testing (simulation) whereas the velocity and acceleration data is zero-centred throughout the test.

6 CONCLUSIONS

In this experimental investigation, subject balance behaviour while walking on both a stationary and laterally oscillating treadmill was investigated with the aid of a 3D motion tracking camera system. The objective was to obtain a better understanding of the root cause or source of the SE GRF, identified in Fig. 5 (d). The approach in this campaign was to investigate the behaviour of a relatively small number of subjects, but in greater detail than has typically been the case in the literature thus far.

The subject's balance response to deck oscillation is dominated by changes to lateral foot placement position. Amplitude modulation from the field of communication theory has been identified as a mathematical analogue for the biomechanical behaviour observed. It has been confirmed that the interaction forces arise directly as a result of the foot placement position, which itself is a function of pedestrian stability. The frequency of gait width modulation was identified as the modulus of the difference between the lateral forcing and deck oscillation frequencies. The underlying reason for this was revealed by examining the subject's CoM oscillation and recognising the influence of a sinusoidally varying inertia force induced by deck motion. Furthermore, the degree to which the subject alters their gait is determined by the degree to which their frontal plane stability is impaired by deck motion. Thus the link between frontal plane balance behaviour and the generation of the SE component of the lateral GRF has been established. Although there is a large degree of ISV, the fundamental HSI mechanism identified, namely periodic gait width modulation resulting in AM of the GRF, can be considered typical for the full test population.

Subject's CoM motion was also found to be well described by the passive dynamics of the IP biomechanical model. Thus active balance control in response to deck motion, (based on

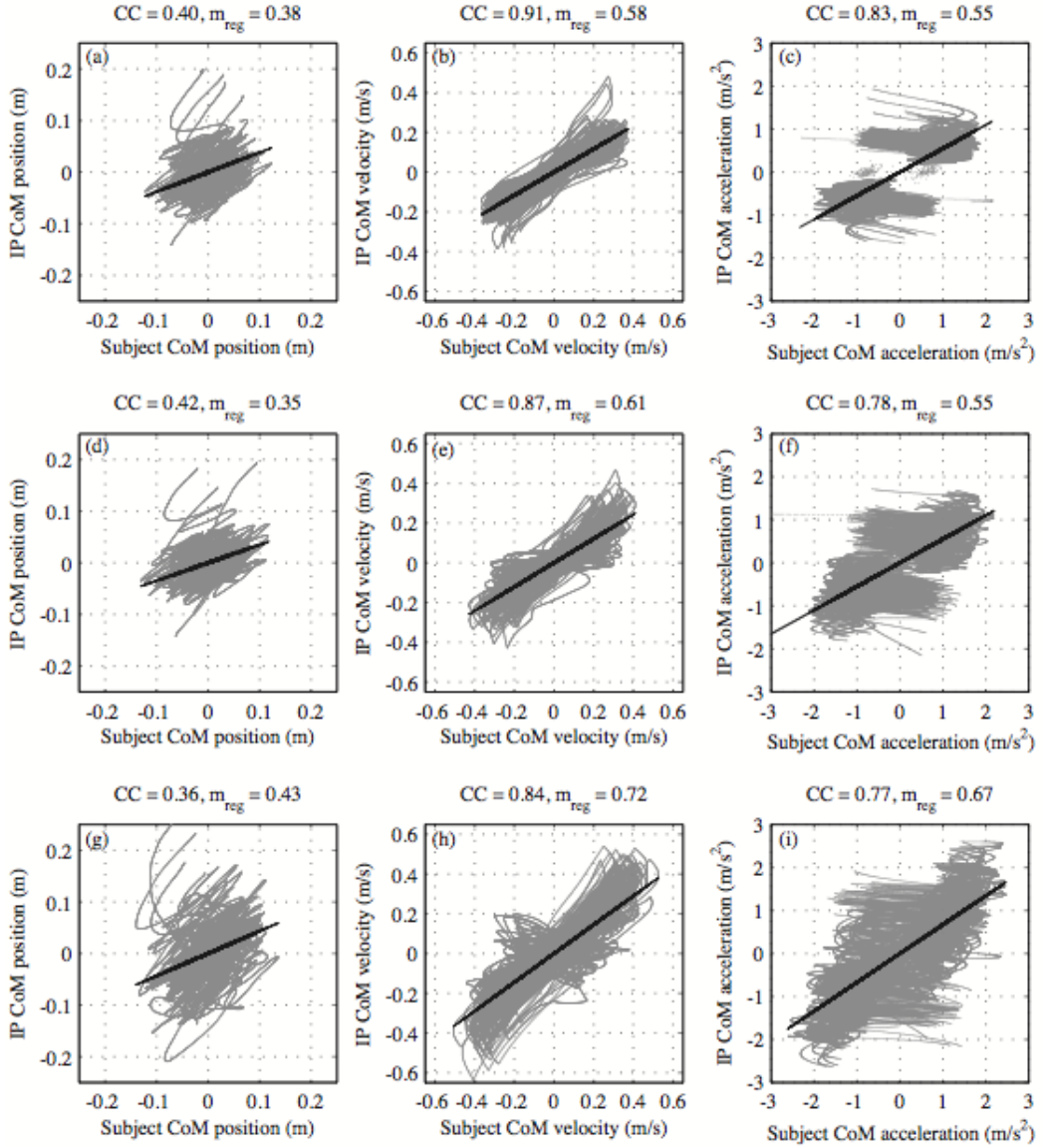

Figure 13: Plot of subject (No. 4) versus equivalent IP behaviour for CoM position (plot a, d, g), velocity (plot b, e, h) and acceleration (plot c, f, i). Plots (a - c) contain all data relating to 5 mm amplitude tests, plots (d - f) contain all data relating to 10 mm amplitude tests and plots (h - i) contain all data relating to 20 mm amplitude tests. Corresponding correlation coefficients are shown above the relevant plot. IP CoP placement based on local CoM velocity.

sensory feedback) does not appear to contribute significantly to the observed CoM motion. In the context of human-induced vibration, the raison d'être of the IP model is to generate GRFs consistent with HSI. In light of the discussion above it can be stated that the gait behaviour simulated is consistent with HSI, i.e. SE forces are simulated through the modulation of IP gait width, Figs. 11. The same mechanism has been confirmed in test subjects under the influence of the identical deck motion.

REFERENCES

[1] J.G.H. Macdonald, Pedestrian-induced vibrations of the Clifton Suspension Bridge, UK, *Proceedings of the ICE - Bridge Engineering*, **161**, 69-77, 2008.

[2] J. Brownjohn, P. Fok, M. Roche, P. Omenzetter, Long span steel pedestrian bridge at Singapore Changi Airport part 2: Crowd loading tests and vibration mitigation measures, *The Structural Engineer*, **82**, 28-34, 2004.

[3] F. Ricciardelli, A. Pizzimenti, Lateral walking-induced forces on footbridges, *Journal of Bridge Engineering*, **6**, 677-688, 2007

[4] E.T. Ingölfsson, C.T. Georgakis, F. Ricciardelli, J. Jönsson, Experimental identification of pedestrian-induced lateral forces on footbridges, *Journal of Sound and Vibration*, **330**, 1265-1284, 2011.

[5] A. Pizzimenti, Analisi sperimentale dei meccanismi di eccitazione laterale delle passerelle ad opera dei pedoni (experimental analysis of the lateral pedestrian-induced mechanism of excitation of footbridges), *Ph.D Thesis*, Department of Civil and Environmental Engineering, University of Catania, 2003

[6] S.P. Carroll, J.S. Owen, M.F.M Hussein, Reproduction of lateral ground reaction forces from visual marker data and analysis of balance response while walking on a laterally oscillating deck, *Engineering Structures*, **49**, 1034-1047, 2013

[7] Charnwood Dynamics Ltd, Leicestershire, UK Coda mpx30 User Guide,

[8] P. deLeva Adjustment to Zatsiorsky-Seluyanov's segment inertia parameters, *Journal of Biomechanics*, **29**, 1223-1230, 1996

[9] A. Hof, M. Gazendam, W. Sinke, The condition for dynamic stability, *Journal of Biomechanics*, **38**, 1-8, 2005.

[10] J.G.H. Macdonald, Lateral excitation of bridges by balancing pedestrians, *Proceedings of the Royal Society a-Mathematical Physical and Engineering Sciences*, **465**, 1055-1073, 2009.

[11] S.P. Carroll, J.S. Owen, M.F.M Hussein, Crowd-bridge interaction by combining biomechanical and discrete element models, In: *Proceedings of the 8th international conference on structural dynamics*, Leuven, 2011

[12] M. Bocian, J.G.H. Macdonald, J. Burn Biomechanically inspired modelling of pedestrian-induced forces on laterally oscillating structures, *Journal of Sound and Vibration*, **331**, 3914-3929, 2012.

[13] S.P. Carroll, J.S. Owen, M.F.M Hussein, A coupled biomechanical/discrete element crowd model of crowd-bridge dynamic interaction & application to the Clifton Suspension Bridge, *Engineering Structures*, **49**, 58-75, 2013